



Magnetic properties and Mössbauer spectra of nanosized CoFe_2O_4 powders

M. Grigorova^a, H.J. Blythe^b, V. Blaskov^c, V. Rusanov^a, V. Petkov^a, V. Masheva^a,
D. Nihtianova^d, Ll.M. Martinez^e, J.S. Muñoz^e, M. Mikhov^{a,f,*}

^aFaculty of Physics, St. Kliment Ohridski, Sofia University, 5 James Bourchier Blvd., 1126-Sofia, Bulgaria

^bPhysics Department, The University of Sheffield, Sheffield, S3 7RH, UK

^cInstitute of General and Inorganic Chemistry, Bulgarian Academy of Sciences, 1113-Sofia, Bulgaria

^dCentral Laboratory of Mineralogy and Crystallography, Bulgarian Academy of Sciences, 1000-Sofia, Bulgaria

^eDepartamento de Física, Universidad Autónoma de Barcelona, 08193 Bellaterra (Barcelona), Spain

^fInstituto de Física – UFRGS, C.P. 15051, 91501-970 Porto Alegre, RS, Brazil

Received 27 June 1997; received in revised form 3 October 1997

Abstract

CoFe_2O_4 fine powders with particle sizes between 43 Å (4.3 nm) and 465 Å (46.5 nm) were produced by a method of ‘gentle’ chemistry. It was found that a surface layer with thickness of about 10 Å does not contribute to the magnetization in the fields used. Maximum coercivity of 14 kOe and reduced remanence of 0.64 were measured at 5 K after magnetization in 50 kOe indicating a cubic-type magnetocrystalline anisotropy. © 1998 Elsevier Science B.V. All rights reserved.

Keywords: Fine particles; Ferrite; Anisotropy – multi-axial; Superparamagnetism

1. Introduction

Co-ferrite has a very high cubic magnetocrystalline anisotropy accompanied by a reasonable saturation magnetization. These properties make it a promising material for use in the production of isotropic permanent magnets, magnetic recording and magnetic fluids. For such applications it is necessary to produce stable single-domain

particles. The room-temperature (RT) single-domain diameter, estimated by the Kittel formula, is 1000 Å and the RT superparamagnetic diameter, estimated by the Néel theory, is 100 Å [1]. The RT critical single-domain size, reported on the basis of coercivity measurements, is of the order of 700 Å [2]. Stoichiometric CoFe_2O_4 is known to have a cubic magnetocrystalline anisotropy with three easy axes, [1 0 0], and temperature dependence of the first anisotropy constant obeying the empirical relation [3]:

$$K = 19.6 \times 10^6 \times \exp(-1.90 \times 10^{-5} \times T^2) \text{ erg/cm}^3.$$

*Corresponding author. Tel.: +359 2 662561; fax: +359 2 689085; e-mail: mikhov@phys.uni-sofia.bg.

The temperature dependence of the saturation magnetization is given by the expression [4]

$$\sigma_s(T) = 93.9 \times (1 - 1.576 \times 10^{-6} \times T^2) \text{ emu/g,}$$

and the density of the bulk material is 5.29 g/cm^3 .

A random system of spherical, non-interacting single-domain particles with cubic anisotropy and the above parameters will have the following saturation magnetization, coercivity and reduced remanence [5,6]:

$$\sigma_s(5 \text{ K}) = 93.9 \text{ emu/g,} \quad \sigma_s(300 \text{ K}) = 80.8 \text{ emu/g,}$$

$$H_c(5 \text{ K}) = 25.2 \text{ kOe,} \quad H_c(300 \text{ K}) = 5.3 \text{ kOe,}$$

$$\frac{\sigma_r}{\sigma_s} = 0.83.$$

A number of non-standard technologies were recently used for producing fine Co-ferrite powders. Most of these are based on chemical reactions [7–11] but some other methods such as mechanical alloying [12] and glass crystallization [13] have also been used. Some of the data on the magnetic properties of fine Co-ferrite powders are summarized in Table 1. One can see that the measured values of saturation magnetization, coercivity and remanence are distributed in broad ranges, but in all cases they are less than the above given

maximum values. The only exceptions are the reduced remanences reported by Davies et al. [9] and Moumen et al. [10] which considerably exceed the value of 0.5. This is an indication that the cubic magnetocrystalline anisotropy is predominant in these particles. However, the maximum magnetization and coercivity reported in Ref. [10], measured at 20 K using fields of up to 50 kOe are still significantly lower than the expected ones. There are no data regarding saturation magnetization or coercivity reported in Ref. [9].

In our previous work [11], Co-ferrite powder was studied which consisted of particles with an average diameter of about 50 Å. The coercivity measured at 5 K after magnetization in a field of 50 kOe slightly exceeds 13 kOe, but the maximum magnetization and reduced remanence were too low. A closer look at Table 1 would suggest that the magnetic characteristics depend not only on the particle size but also on the method of preparation.

The purpose of the present work is to investigate, in a systematic manner, the principal magnetic properties of a series of Co-ferrite powders consisting of fine particles with progressively increasing sizes, produced by the co-precipitation from cobalt–iron hydroxide carbonate solutions followed by annealing at relatively low temperatures.

Table 1

Some data on the magnetic properties of CoFe_2O_4 fine powders found in the literature. The units are quoted as in the references

| Particle size | σ_s | σ_r/σ_s | H_c | Preparation technique | Ref. |
|---|--|--|---|-------------------------------|------|
| 26–210 nm | 78–88 ^a Am ² /kg (RT) | 0.3–0.4 | 41–71 kA/m ^b | Glass-cryst. | [13] |
| 30 nm | 77 emu/g (RT) | — | 2–2.7 kOe | Mech. all. & anneal. 750°C | [12] |
| 2–5 nm | 50 emu/g (20 K) | 0.74 | 8.8 kOe | Chemical | [10] |
| 16 Å (X-ray) 20–40 Å (TEM) in magn. fluid | — | 0.83($T \rightarrow 0$) 0.78(4.2 K) | — | Hydrotherm. growth | [9] |
| 160 Å | 70 emu/g | — | ≤ 10 kOe (77 K) 750 Oe (300 K) | Hydrotherm. growth | [7] |
| 50 Å | 15 emu/g (5 K) | 0.36 | 13 kOe | Chemical | [11] |

^a (74–88) emu/g.

^b (515–892) Oe.

2. Experimental

The fine powders of CoFe_2O_4 were synthesized following the method described in Ref. [14]. The initial cobalt–iron hydroxide carbonate was obtained by co-precipitation from Fe(II) and Co(II) solutions, with the Me(II) concentration being 0.6 mol/dm^3 . The precipitates were washed until no more Cl^- ions were detected. Isothermal calcination continued for 6 h at different annealing temperatures T_A – 325°C , 345°C , 370°C , 545°C and 700°C .

The X-ray characterization of the samples was carried out on an automated powder diffractometer using Co K_α radiation. TEM investigations were performed using a Philips EM 420-T in routine mode. The Mössbauer spectra were recorded at 80 and 300 K with a conventional constant acceleration spectrometer combined with a multi-channel analyser. A source of $^{57}\text{Co}(\text{Rh})$ with activity of about 50 mCi was used. The isomer shifts (IS) were referred to $\alpha\text{-Fe}$. A NaI(Tl) scintillation detector with a crystal of 0.1 mm thickness was used to detect the Mössbauer quanta (14.4 keV). The Mössbauer spectra were computer processed and decomposed to single Lorentzians (when it was possible) by a fitting program using a least-squares method.

AC magnetic susceptibility was measured between 6 and 300 K in a field of 1 Oe at a frequency of 111.1 Hz using a Lake-Shore susceptometer. Magnetizations in the temperature range 77–820 K and in fields up to 5 kOe were measured using a vibrating sample magnetometer. Magnetizations between 5 and 300 K and in fields up to 50 kOe were measured using a Quantum Design SQUID magnetometer. The samples for magnetic measurements were prepared by pressing the powder into plastic or quartz tubes so that the particles could not move during measurements. Some of the samples for the SQUID experiments were prepared by mixing the powders with a low-temperature Araldite.

3. Results and discussion

The main experimental data for the samples studied are summarized in Table 2.

3.1. Structure and morphology

X-ray diffraction patterns of all the samples are shown in Fig. 1. All peaks correspond to a cubic, spinel-type lattice (Fd3m) with lattice parameter $a = 8.20(5) \text{ \AA}$. There were no detectable traces of extra crystalline or amorphous phases present. The crystal structure was fully confirmed by selected area electron diffraction (SAED).

The X-ray diffraction peaks for the powder produced at the lowest annealing temperature ($T_A = 325^\circ\text{C}$) are fairly broad, indicating that the sample consists of quite fine crystallites. These line broadenings for the other samples decrease with increase in the temperature of anneal. The full-widths at half-maximums of (1 1 1), (1 1 0) and (1 0 0) diffraction peaks were used for the estimation of crystallite diameters, $D(hkl)$, along these directions and the mean values of the particle diameters $\langle D \rangle_{\text{X-ray}}$ given in Table 2. As is shown in Fig. 2 the mean particle size increases almost exponentially with the annealing temperature.

Typical morphologies of the CoFe_2O_4 particles visualized by TEM are shown in Fig. 3. As can be seen from Fig. 3a, the powder prepared by calcination at the lower temperature of 345°C consists of platelets with fine granular microstructure. In the powder prepared by calcination at the higher temperature of 545°C , the grains in the platelets are larger, more separated and some of the platelets have already been destroyed; the shape of the grains is almost spherical (Fig. 3b). The grain diameters, obtained by TEM, agree with those estimated from the X-ray powder diffraction peaks.

3.2. Mössbauer spectra

The Mössbauer spectra of all the samples measured at 300 and 80 K shown in Figs. 4 and 5. The RT spectra change from a paramagnetic doublet for the smallest particles (Fig. 4a) to a well-resolved sextet with somewhat broadened lines for the largest ones (Fig. 4e). Two sub-spectra with effective fields of $H_{\text{eff}} = 491$ and 497 kOe , corresponding to Fe^{3+} ions in B and A sites can be distinguished in the latter case. The low-temperature spectra are magnetically split for all the samples. The spectrum for the largest particles, shown in Fig. 5e can be

Table 2

The main experimental data for the fine CoFe_2O_4 powders, annealed at different temperature T_A

| T_A (°C) | Part. size D (Å) ($\pm 10\%$) | T_B (K) | $T = 300$ K | | | | $T = 5$ K | | | |
|------------|---|-----------|--------------------|--------------------|-------------|---------------------|---------------------|--------------------|-------------|---------------------|
| | | | σ_m (emu/g) | σ_r (emu/g) | H_c (kOe) | σ_r/σ_m | σ_m (emu/g) | σ_r (emu/g) | H_c (kOe) | σ_r/σ_m |
| 325 | 47 (1 1 1) | 250 | 13 | — | — | — | 14.9 ^{ZFC} | 5.4 | 13.2 | 0.36 |
| | 37 (1 1 0) | | | | | | 17.35 ^{FC} | | | |
| | 45 (1 0 0) | | | | | | | | | |
| | $\langle 43 \rangle_{\text{X-ray}}$ $\langle 65 \rangle_{\text{TB}}$ | | | | | | | | | |
| 345 | 51 (1 1 1) | 275 | 16.4 | — | — | — | 18.2 ^{ZFC} | 7.3 | 14.1 | 0.4 |
| | 38 (1 1 0) | | | | | | 21.1 ^{FC} | | | |
| | 63 (1 0 0) | | | | | | | | | |
| | $\langle 51 \rangle_{\text{X-ray}}$ $\langle 73 \rangle_{\text{TB}}$ | | | | | | | | | |
| 370 | 53 (1 1 1) | 26.6 | 0.4 | 0.071 | 0.01(5) | 0.01(5) | 29.5 ^{ZFC} | 15 | 14.0 | 0.51 |
| | 49 (1 1 0) | | | | | | 31.4 ^{FC} | | | |
| | 95(1 0 0) | | | | | | | | | |
| | $\langle 66 \rangle_{\text{X-ray}}$ | | | | | | | | | |
| 545 | 171 (1 1 1) | 473 | 52.2 | 10.4(6) | 0.920 | 0.19 | 62.0 ^{ZFC} | 38.3 | 13.2 | 0.62 |
| | 163 (1 1 0) | | | | | | 63.1 ^{FC} | | | |
| | 251 (1 0 0) | | | | | | | | | |
| | $\langle 195 \rangle_{\text{X-ray}}$ $\langle 223 \rangle_{\text{TB}}$ | | | | | | | | | |
| 700 | 394 (1 1 1) | 623 | 67.1 | 22.9 | 1.750 | 0.34 | 74.8 ^{ZFC} | 47.5 | 10.0 | 0.64 |
| | 411 (1 1 0) | | | | | | 75.0 ^{FC} | | | |
| | 591 (1 0 0) | | | | | | | | | |
| | $\langle 465 \rangle_{\text{X-ray}}$ $\langle 694 \rangle_{\text{TB}}$ | | | | | | | | | |

Note: $\langle D \rangle$ indicate the mean crystallite sizes. $\sigma_{\text{max}}^{\text{ZFC}}$ and $\sigma_{\text{max}}^{\text{FC}}$ are measured in a field of 50 kOe in zero-field-cooled (ZFC) and field-cooled (FC) regimes, respectively.

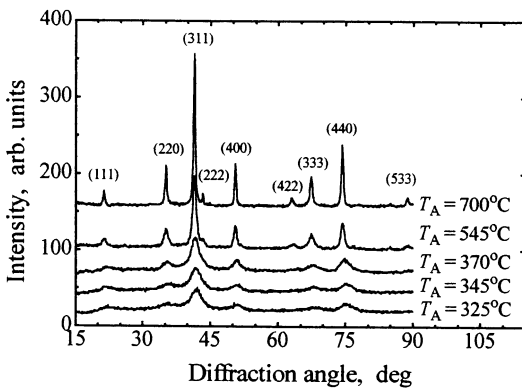


Fig. 1. X-ray diffraction patterns obtained using CoK_α radiation of CoFe_2O_4 powders annealed at different temperatures.

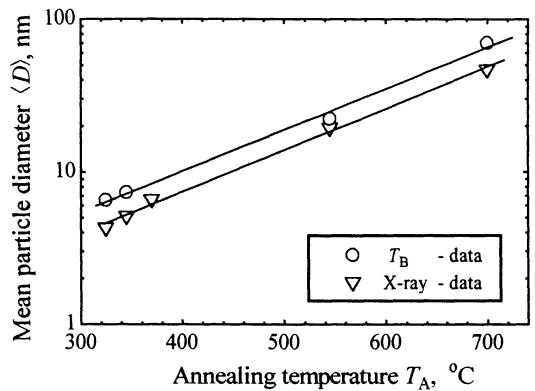


Fig. 2. Annealing temperature dependence of particle diameters estimated from broadening of X-ray diffraction peaks and from mean blocking temperatures.

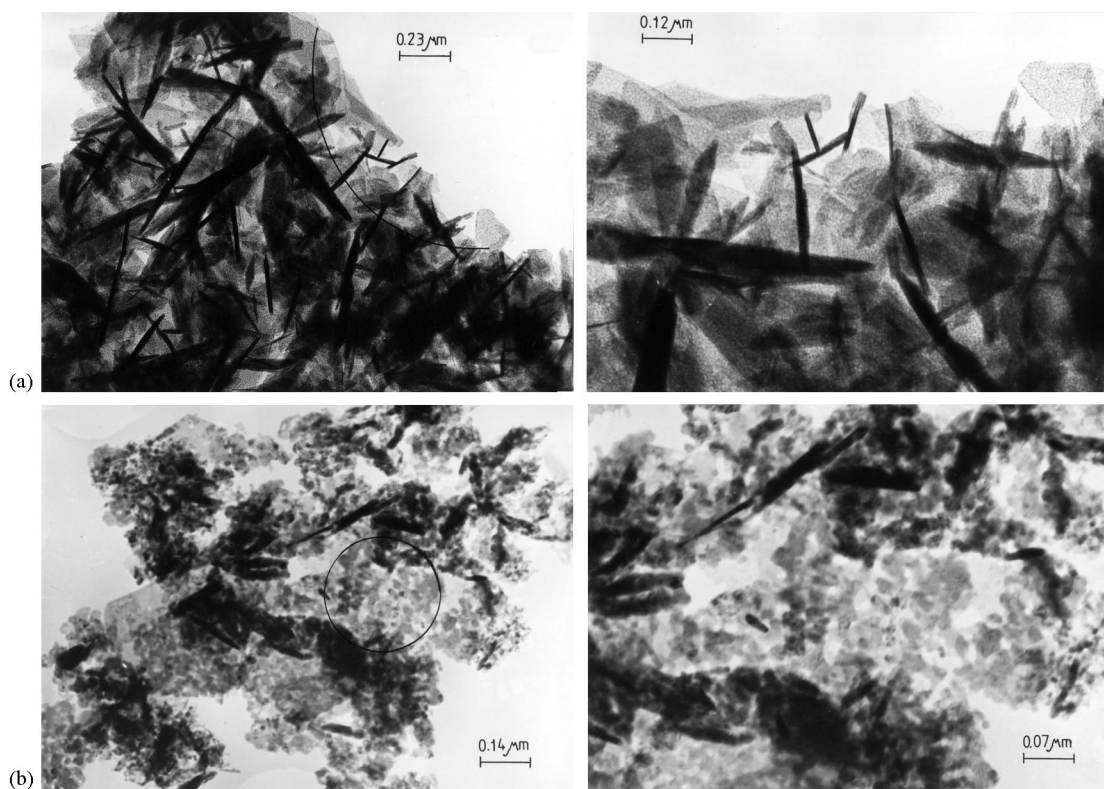


Fig. 3. Bright field micrographs of CoFe_2O_4 powder annealed at (a) 345°C , and (b) 545°C . The pictures on the right-hand side represent the enlarged areas marked.

fitted with two well-defined sextets corresponding to Fe^{3+} ions in B and A sites. The Mössbauer parameters for A sites are: isomer shift (related to $\alpha\text{-Fe}$), $\text{IS} = 0.512$ mm/s; quadruple splitting, $\text{QS} = 0.037$ mm/s; effective magnetic field, $H_{\text{eff}} = 543$ kOe; and relative intensity, $I_{\text{rel}} = 47\%$. The corresponding parameters for B sites are $\text{IS} = 0.396$ mm/s, $\text{QS} = 0.013$ mm/s, $H_{\text{eff}} = 513$ kOe and $I_{\text{rel}} = 53\%$. The Mössbauer lines are of normal width of 0.25–0.3 mm/s indicating almost ideal inverse spinel structure. The Co^{2+} cation distribution estimated from this spectrum is



which means that the concentration of Co^{2+} ions in B-sites is very close to 1. This result is in a good agreement with the results reported in Ref. [15] for a well-relaxed polycrystalline CoFe_2O_4 sample.

The structure of the last two lines of spectrum shown in Fig. 5e is noticeable. We tried to fit them with two or three sub-lines as shown in Fig. 6a and Fig. 6b, respectively, and the three-sub-lines fit is much better than the two-sub-lines one. These three sub-lines, marked in Fig. 6 as A, B(6) and B(5) could be related to (i) Fe^{3+} ions occupied A-sites; (ii) Fe^{3+} ions occupied B-sites surrounded by six Fe^{3+} ions in A-sites; and (iii) Fe^{3+} ions occupied B-sites surrounded by five Fe^{3+} ions in A-sites and one Co^{2+} ion in A-site.

The following conclusions can be drawn from the Mössbauer investigations. The magnetic state of the powders at RT change from a superparamagnetic to a ferrimagnetic one with increase of the annealing temperature. The lines for the powder annealed at the highest temperature of 700°C are somewhat broadened indicating that the state is not a pure ferrimagnetic one. The magnetic state of

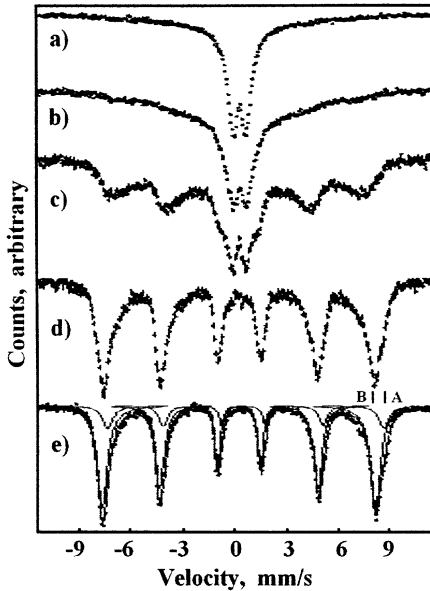


Fig. 4. Mössbauer spectra, obtained at 300 K for CoFe_2O_4 powders annealed at (a) 325°C, (b) 345°C, (c) 370°C, (d) 545°C, and (e) 700°C.

the powders at 80 K changes from partly ferrimagnetic to a well-defined ferrimagnetic one and the sample annealed at the highest temperature of 700°C has almost ideal inverse spinel structure.

3.3. Magnetic measurements data

The temperature dependences of both the AC and DC magnetic susceptibilities, χ_{ac} and χ_{dc} , measured in fields of different strengths and frequencies exhibit typical superparamagnetic behaviour, similar to that reported in Ref. [9]. The mean blocking temperatures $\langle T_B \rangle$, measured as the temperatures at which $\chi(T)$ have their maxima, increase with increase of the annealing temperature, and thus with increase of particle size. $\langle T_B \rangle$ exceeds 300 K for the powders annealed at temperatures 370°C, 545°C and 700°C. The mean volumes $\langle V \rangle$ of the particles, assumed to be superparamagnetic were estimated by the well-known relation

$$K_1(T_B) \times \langle V \rangle \approx 25 \times k_B \times \langle T_B \rangle$$

(k_B is the Boltzmann constant). The mean particle diameters calculated in this manner show the same

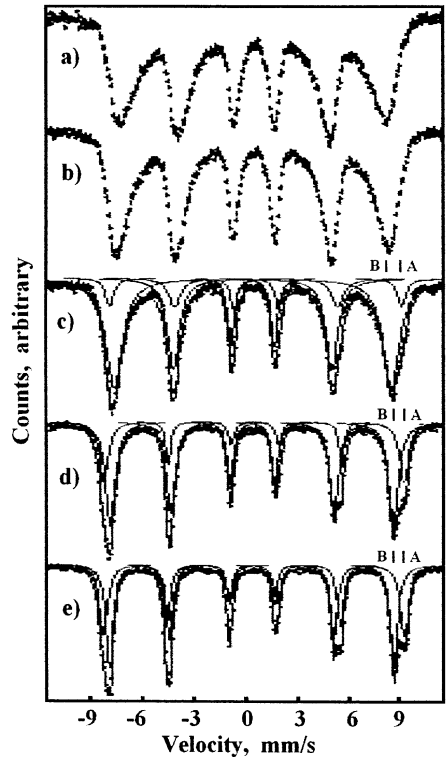


Fig. 5. Mössbauer spectra, obtained at 80 K for CoFe_2O_4 powders annealed at (a) 325°C, (b) 345°C, (c) 370°C, (d) 545°C, and (e) 700°C.

dependence on annealing temperature as the diameters estimated from X-ray data. However, they are somewhat larger than the final results as shown in Fig. 2.

Initial magnetization curves of thermally demagnetized samples and hysteresis loops were measured at 5 and 300 K in fields up to 50 kOe for all samples, although only the data for samples with the smallest and the largest particles sizes are plotted in Fig. 7a and Fig. 7b.

The distinguishable hysteresis phenomena at RT appear only for the samples annealed at temperatures 370°C, 545°C and 700°C. The samples annealed at lower temperatures behave superparamagnetically at RT as shown in Fig. 7a. These results coincide with the low-field $\chi(T)$ measurements already discussed. Superparamagnetic behaviour of the sample annealed at 325°C is additionally confirmed by the coincidence of the

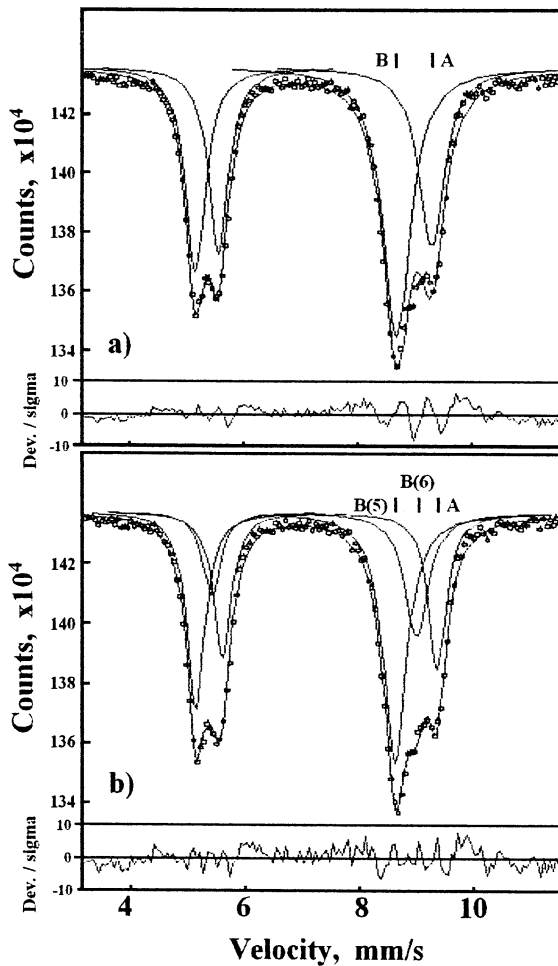


Fig. 6. Fifth and sixth Mössbauer lines obtained at 80 K for CoFe_2O_4 powder annealed at 700°C , fitted with (a) two, and (b) three sub-lines.

σ versus H/T plots for different temperatures shown in Fig. 8. This reduced plot is also in agreement with the classical s vs. H/T plots [16]. The curves are coincident to within about $\pm 5\%$. The discrepancies observed could be mainly related to the particle-size distribution, which becomes important near the blocking temperature.

3.3.1. Magnetic properties at 5 K

The maximum magnetizations measured at 5 K in field of 50 kOe are lower than for the bulk material and they increase with increase of annealing

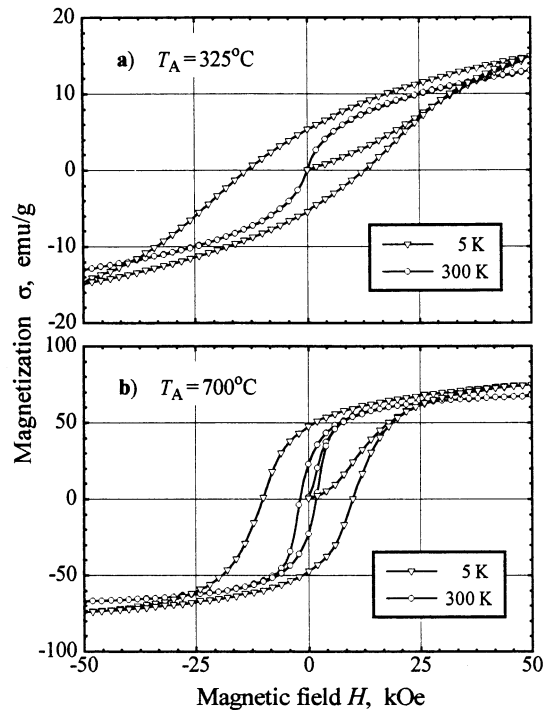


Fig. 7. Initial magnetization curves and hysteresis loops at 5 and 300 K plotted for CoFe_2O_4 powders annealed at (a) 325°C , and (b) 700°C .

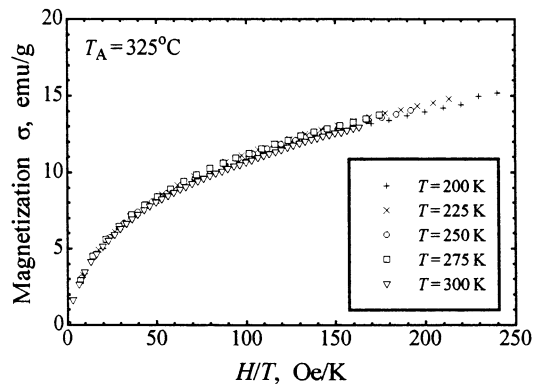


Fig. 8. Magnetization vs. H/T curves plotted at different temperatures for CoFe_2O_4 powder annealed at 325°C .

temperature (and particle size). The high magnetic anisotropy could not be considered as a main reason for this reduction of magnetization since the difference between the maximum magnetization

measured in the zero-field-cooled (ZFC) and field-cooled (FC) regimes is less than 15% for the smallest particle size and decreases to zero for the largest ones. The reduction of maximum magnetization could be related to the existence, for each particle, of a surface layer in which magnetic moments do not contribute to the magnetization in the field applied. Let the volume of this surface layer be V_s and the total volume of the particle be V . Thus the effective ‘magnetic volume’ of the particle is $V_m = V - V_s$. In the idealized case the ratio between the ‘magnetic’ and total volumes of the particle will be equal to the ratio between the measured magnetization, $\sigma_{\max}(T, H)$, and the magnetization of the bulk material expected for the same temperature and magnetic field, $\sigma_{\text{bulk}}(T, H)$:

$$\frac{V_m}{V_m + V_s} = \frac{\sigma_{\max}}{\sigma_{\text{bulk}}}$$

By using the above quoted values for saturation magnetization and first anisotropy constant for bulk CoFe_2O_4 , and assuming the particles as spherical once, the thickness of such a ‘dead’ surface layer at 5 K is estimated to be

$$d_s = (10 \pm 1.5)\text{\AA}$$

This value is in a reasonable agreement with the data reported for small particles of Ba–ferrite [17] and Co–ferrite [8,18] as well as with a recently developed model [19]. Under this assumption the magnetization of the ‘magnetic cores’ of the particles in a field of 50 kOe is 89.57 emu/g; this does not depend on the particle size.

The coercivities measured at 5 K after ZFC magnetization in a field of 50 kOe for the samples with different mean particle sizes are given in Fig. 9. Although, they are higher than the coercivities reported in the available literature, they are still a factor of two lower than the theoretically expected ones and they decrease slightly with increasing particle size. Simultaneously, the reduced remanence increases with increasing particle size, exceeding the value of 0.5 as shown in Fig. 9. For the sample annealed at 700°C with mean particle size of $\langle D \rangle_{\text{X-ray}} = 465 \text{\AA}$, the reduced remanence reaches a value of 0.64, indicating that the cubic-type magnetic anisotropy is significant in these particles. We

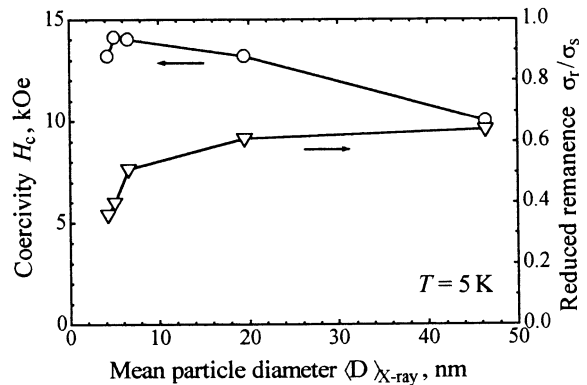


Fig. 9. Dependences of the coercivity and reduced remanence measured at 5 K on mean particle diameter.

should like to point out that the above data on reduced remanence were obtained without taking into account the demagnetization field, since it is difficult to do this in a proper manner for the present fine particle samples. In any case, some demagnetization fields exist and this will shift the magnetization curves toward the lowest fields, this way increasing the reduced remanences, so that the values measured have to be considered as the lowest possible values.

The combination of coercivity, decreasing with increase of particle size (and annealing temperature), and remanence, increasing with increase of particle size (and annealing temperature) is rather unusual. One possible explanation could be as follows.

For the samples annealed at lower temperatures, the single-domain particles are smaller, with higher internal strains; they are closely packed in the plates, as observed in TEM pictures (see Fig. 3a). The internal strains lead to the existence of uniaxial magnetic anisotropy in addition to the cubic magnetocrystalline anisotropy, which originated from the cubic crystal structure. The close packing favours the existence of closed magnetic circuits and possibly also of some ‘fanning’-like modes of magnetization. Thus, the magnetic behaviour of the system is far from that of the behaviour expected for non-interacting single-domain particles with cubic anisotropy.

On increasing the annealing temperature, the particles grow larger and the contribution of the

uniaxial anisotropy due to the internal strains diminishes, their anisotropy approaches the cubic type value, which leads to a decrease of H_c . Simultaneously, the particles separate from each other as can be seen from Fig. 3b. In this way, the contribution of the closed magnetic circuits and the ‘fanning’-like modes of magnetization decreases and the magnetic behaviour of the system approaches that of a random system of non-interacting single-domain particles with cubic anisotropy, exhibiting values of reduced remanence greater than 0.5. It is still not clear why the absolute values of coercivity is about a factor of two lower than the value expected.

3.3.2. Magnetic properties at 300 K

As already mentioned, only the powders annealed at higher temperatures (370°C, 545°C and 700°C) exhibit hysteresis phenomena at room temperatures. The coercivities and the reduced remanences are shown in Fig. 10. Their values increase with increase of the annealing temperature (and particle size) but they are somewhat lower than the predicted values. This could be related to the presence of some superparamagnetic particles in the samples and this concentration decreases with increasing of annealing temperature. As shown in Fig. 11 the size dependence of coercivity is similar to that reported in Ref. [2]. Figs. 10 and 11 show that the coercivity and reduced remanence, both increasing with particle size, are far from their

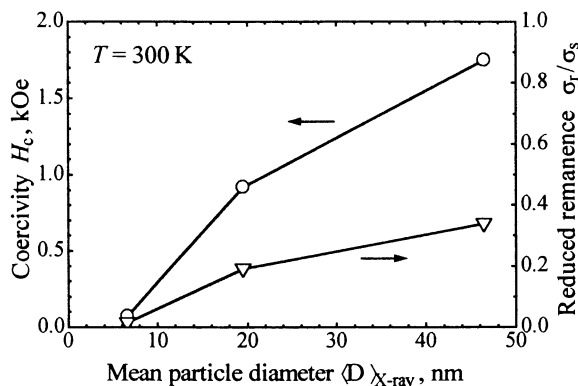


Fig. 10. Dependences of the coercivity and reduced remanence measured at 300 K on mean particle diameter.

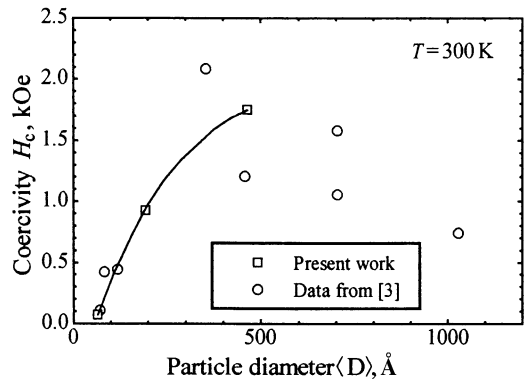


Fig. 11. Dependences of the coercivity at 300 K on mean particle diameter, and compared with the data reported in Ref. [3].

‘saturated’ values and the technology used for their preparation permits the production of powders with higher hysteresis parameters.

4. Conclusions

Fine CoFe_2O_4 particles have been produced by co-precipitation from Fe(II) and Co(II) solutions followed by a relatively low-temperature anneal; the mean particle size can be controlled by the temperature of annealing. At lower annealing temperature, the particles are nano-sized and closely packed in the form of platelets with micron sizes. With increase of annealing temperature the particles grow larger and start to separate from each other. The highest coercivity of 14.1 kOe has been measured at 5 K for the smallest particles. The highest reduced remanence of 0.64 at 5 K has been observed for the largest particles, indicating an existence of multi-axial anisotropy. The room-temperature hysteresis parameters are somewhat lower due to the existence of superparamagnetic phase even in the powders annealed at highest temperature.

Acknowledgements

This work was supported by the Bulgarian Foundation for Scientific Investigations under contract Φ -453/1994. The authors are obliged to

Dr. J. Geshev for critical reading the manuscript and for the figures processing.

References

- [1] D.J. Dunlop, *Phil. Mag. Ser. 19* (1969) 239.
- [2] A.E. Berkowitz, W.J. Schuele, *J. Appl. Phys.* 30 (1959) 134S.
- [3] H. Shenker, *Phys. Rev.* 107 (1957) 1246.
- [4] R. Pauthenet, *Ann. Phys.* 7 (1952) 710.
- [5] E.W. Lee, J.E.L. Bishop, *Proc. Phys. Soc.* 89 (1966) 661.
- [6] J. Geshev, O. Popov, V. Masheva, M. Mikhov, *J. Magn. Magn. Mater.* 92 (1990) 185.
- [7] W.J. Schuele, V.D. Deetscreek, *J. Appl. Phys.* 32 (1961) 235S.
- [8] B. Hannoyer, L. Presmanes, P. Tailhades, A. Rousset, Italian Physical Society Conf. Proc., 'ICAME-95', Rimini, 10–16 September 1995, vol. 50, p. 295.
- [9] K.J. Davies, S. Wells, R.V. Upadhyly, S.W. Charles, K. O'Grady, M. El Hilo, T. Meaz, S. Mørup, *J. Magn. Magn. Mater.* 149 (1995) 14.
- [10] N. Moumen, P. Veillet, M.P. Pileni, *J. Magn. Magn. Mater.* 149 (1995) 67.
- [11] V. Blaskov, V. Petkov, V. Rusanov, Ll.M. Martinez, B. Martinez, J.S. Muñoz, M. Mikhov, *J. Magn. Magn. Mater.* 162 (1996) 331.
- [12] J. Ding, P.G. McCormick, R. Street, *Solid. State Commun.* 95 (1995) 31.
- [13] R. Müller, W. Schüppel, *J. Magn. Magn. Mater.* 155 (1996) 110.
- [14] E. Uzunova, D. Klissurski, I. Mitov, P. Stefanov, *Chem. Mater.* 5 (1993) 576.
- [15] G.A. Sawatzky, F. Van Der Woude, A.H. Morrish, *Phys. Rev.* 187 (1969) 747.
- [16] I.S. Jacobs, C.P. Bean, in: G.T. Rado, H.Suhl (eds.), 'Magnetism', vol. III, Academic Press, New York, 1993, p. 270.
- [17] X. Batlle, X. Obradors, M. Medarde, J. Rodríguez-Carvajal, M. Pernet, M. Vallet-Regí, *J. Magn. Magn. Mater.* 124 (1993) 228.
- [18] P. Mollard, P. Germe, A. Rousset, *Physica B* 86–88 (1977) 1393.
- [19] R.H. Kodama, A.E. Berkowitz, E.J. McNiff, S. Foner, *Phys. Rev. Lett.* 77 (1996) 394.